RSC Publishing Faraday Discussions

Selectivity and polarization in water channel membranes: lessons learned from polymeric membranes and CNTs

Journal:	*Faraday Discussions*
Manuscript ID	FD-ART-03-2018-000054.R1
Article Type:	Paper
Date Submitted by the Author:	24-Mar-2018
Complete List of Authors:	Freger, Viatcheslav; Technion - Israel Institute of Technology, Wolfson Department of Chemical Engineering ; Technion - Israel Institute of Technology, Grand Technion Energy Program ; Technion - Israel Institute of Technology, Russel Berrie Nanotechnology Institute

SCHOLARONE™
Manuscripts

Table of Content Entry

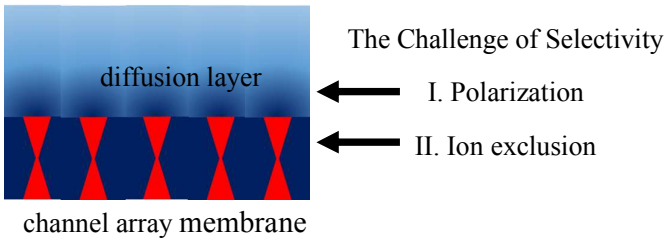

The aspects of ion exclusion and concentration polarization are highlighted as critical for achieving high selectivity in artificial water channel

Faraday Discussions

ARTICLE

Selectivity and polarization in water channel membranes: lessons learned from polymeric membranes and CNTs

Viatcheslav Freger*[a]

eceived 00th January 20xx,
Accepted 00th January 20xx

DOI: 10.1039/x0xx00000x

www.rsc.org/

Water channels are employed by Nature to move pure water across cell membranes, while selectively rejecting salts. At present, synthetic channels successfully mimic water permeation, yet even best channels, such as carbon nanotubes (CNT) and graphene oxide stacks, still fall short of the selectivity target. The present paper analyzes factors that may help enhance and control salt rejection, based on the lessons learned from conventional membranes and CNTs. First, it highlights the importance of raising the ion self-energy (dielectric mechanism), which suggests that having the channels both narrow and surrounded by a low-dielectric environment is key to high selectivity. In contrast, pore charge alone is insufficient, yet it may help enhance and tune ion rejection, provided non-mean-field effects enhanced in low-dielectric pores, such as ion association and sorption, especially of H+ and OH- ions, are properly understood and addressed in the channel design. Second, the role of concentration polarization (CP) is analyzed, which shows that the CP level is apparently small in isolated channels or microscopically small membranes. However, the geometry of the diffusion field should change and CP increase drastically in macroscopic membranes incorporating densely spaced channel arrays. If not properly addressed in membrane design, the increased CP level in scaled-up channel-based membranes may significantly compromise the observed selectivity and require that the target of selectivity be re-set to a still more challenging value. These points may help guide future development of high-performance artificial water channels and their scale-up towards utilization in next-generation water purification membranes..

1. Introduction

Nature employs water channel proteins (aquaporins) to purify water to a high degree by rapidly shuttling it across the membranes as well as preventing ions from doing so. The high selectivity of water channels is due to highly optimized chemistry, charge and geometry of the channels.[1] While biomimetic and synthetic channels mimic permeation rates of water,[2-6] achieving the selectivity levels, commensurate with that of aquaporins in their native environment, seems far more challenging at present. For instance, the current state-of-the-art for CNT porins[2, 6-8] and graphene oxide channels[9] shows salt rejection that barely exceeds 90% even for best rejected divalent ions. The ultrahigh permeability may show diminishing benefits when increased much beyond the current level.[10] On the other hand, enhanced selectivity may offer clear benefit for current technology. [11]

At present, it is clear that ion rejection consistently improves when channel size is reduced.[2, 6] Such results are commonly interpreted in a qualitative way, by assuming that the size of the hydrated ion is the threshold pore size, at which ion rejection becomes significant.[9, 12] However, insights obtained by molecular dynamics (MD) simulations reveal physical mechanisms of transport and selectivity in channels and membranes that are more complex.[13-16] Unfortunately, it is not always straightforward to extrapolate conclusions from MD to real experimental conditions and settings, which often differ from those used in simulations. In this respect, simplified models and arguments that can still capture the underlying physics and transparently explain the observed trends might be of much value for quantifying the pore size effect and formulating practically useful criteria. In particular, such simple theories would also help address the critical question of whether the desired level of ion rejection is achievable for realistic pore widths and in realistic designs and setups.

This paper will highlight lessons recently learned from studies of polymeric desalination membranes and CNT channels that may apply to water channels in general. One lesson is concerned with the mechanism of selectivity, mainly related to the exclusion of ions from the pore. In this respect, the paper will emphasize the role of dielectric mechanism, which acts through increasing the self-energy of an ion in the channel, rather than its interaction with other charges.[17-20] This mechanism is strongly pore- and ion-size-dependent and may be easily mistaken for a steric effect, despite being distinctly different. It allows stronger and more robust ion exclusion than commonly considered repulsion by charged groups located at the pore walls. The dielectric exclusion may however complicate the picture, promoting non-trivial effects such as ion

[a] Technion - Israel Institute of Technology, Wolfson Department of Chemical Engineering, Haifa, 32000, Israel. E-mail: vfreger@technion.ac.il

This journal is © The Royal Society of Chemistry 20xx

binding and association, which might both suppress and enhance salt permeation.

The second point highlighted in the paper is concerned with the effect of mass transfer limitations. This effect is associated with the solution adjacent to the membrane, collectively referred to as concentration polarization. We will show that, without properly considering this limitation, extrapolating the performance of individual channels to large channel arrays may significantly overestimate the performance. Ignoring such limitations may largely underestimate the challenges of developing macroscopic membranes based on artificial channels and, especially, meeting the target selectivity.

2. The mechanisms of selectivity and ion exclusion

2.1. Diffusivity and sorption selectivity factors

Similar to membranes,[21] the selectivity of a channel may be quantified as the selectivity factor defined as the ratio of permeabilities to salt (s) and water (w)

$$\alpha_P = \frac{P_s}{P_w} = \frac{D_s}{D_w} \times \frac{\Gamma_s}{\Gamma_w} = \alpha_D \alpha_\Gamma \quad (1)$$

Here and below the permeabilities P_s and P_w are *not* necessarily normalized to thickness and/or area, however, their ratio α_P is an intrinsic material property, since the geometry cancels out in (1). Equation (1) breaks α_P down to diffusive and sorption factors, defined as the corresponding ratios of the diffusion (D) and partitioning (Γ) coefficients of the permeants. Note that, in absence of a net electric current, salts will always permeate as neutral combinations of their constitutive ions, therefore, salt permeability will derive from ion permeabilities and limited by the least permeable ion of the salt.

The target value of salt-water selectivity α_P of the water channels should be of the order 10^{-5}, typical of today's reverse osmosis membranes (see Section 3). It seems unlikely to achieve such a low value through the diffusion factor α_D, since the relevant permeant radii are not sufficiently different. Admittedly, there is an uncertainty as to which type of radius, e.g., hydrated or bare, would be most appropriate for assessing diffusivity in channels through Stokes-Einstein relation. Moreover, the most appropriate radii may differ for different phenomena, e.g., diffusion and sorption. Nevertheless, all types of radii for most abundant inorganic ions, Na^+, K^+, Ca^{2+}, Mg^{2+}, Cl^- and SO_4^{2-} fall between 0.08 to 0.23 nm, the only exceptions being the Stokes radii of Ca^{2+} (0.31 nm) and Mg^{2+} (0.347 nm) in water.[21] Since the bare radii of Ca^{2+} and Mg^{2+} are under 0.11 nm, the large Stokes radii reflect strong hydration in water, yet in a channel it may not be as strong thereby Stokes radii may be closer to the bare radii.

Further, the size of water molecules is similarly uncertain and may range from 0.1 nm, the Stokes radius deduced from water self-diffusion, to about 0.14 nm, the mean van der Waals radius deduced from electronic structure and interpolated crystallographic data for different oxygen-containing ions.[22, 23] Then, when it comes to transport through water channels, all ion sizes not much different from the size of the water molecule. Considering the similar size for ions and water and, as importantly, the fact that many artificial water channels are significantly larger, the diffusion selectivity factor is unlikely to be significant. Moreover, trying to enhance this factor by tightening the channels down to the size of the ions and water may compromise water permeability [13] and is probably not the right way to go.

Very low values of α_P are then more likely to be achieved via α_Γ. Since water is supposed to fill channels, $\Gamma_w \sim 1$ hence the sorption selectivity is to be controlled mainly by the salt (ion) partitioning. Ultimately, this sets Γ_s as the key parameter. The next section briefly reviews the main mechanisms that control Γ_s in synthetic memrbanes.

2.2. The three ion exclusion mechanisms

The picture of ion exclusion currently adopted in polymeric membranes considers three distinct physical mechanisms.[20, 24-27] The first is *steric exclusion*, not unique to ions, which is an entropic effect, whereby permeant molecules confined in a pore or free-volume cavity increasingly lose their freedom, when the pore and permeant sizes become close. However, it is a relatively weak effect, unless the permeant very closely fit the pores. For instance, the Ferry model including translational entropy only[28] predicts that already a modest steric partitioning coefficient $\Phi = 0.1$ will require not more than 32% difference between the pore and solute radii. A good steric separation then requires that permeants significantly differ in size and the pores be exceptionally rigid and uniform, sharply differentiating between the permeants. This, just as low α_D, might be too difficult to achieve for water and ions.

The second mechanism is the *Donnan exclusion*, arising from the interaction with fixed charged groups present in the membrane. The classical Donnan model considers an ideal solution of ions in the membrane and a smeared uniform *mean-field* Donnan potential, collectively imposed by the fixed charges on all ions to enforce electroneutrality of the membrane phase. Such idealized model ignores screening of the fixed charges and thus overestimates the strength of charge exclusion, i.e., for a given fixed charge density the actual Γ_s will always be higher than the Γ_s predicted by the ideal Donnan model.

In contrast to the Donnan exclusion that considers inter-ionic interactions, the third mechanism, *dielectric exclusion*, originates from the ion solvation in the medium, i.e., ion self-energy *W*. This energy is always positive and large for non-polar low-dielectric media or nanopores in a low-dielectric matrix. The exclusion then follows from the positive self-energy difference ΔW between membrane and solution phases.

One may write down a *mean-field* relation incorporating all three mechanisms, Steric, Donnan and-diElelctric (SDE), and relate Γ_s of the invading free salt (i.e., co-ions) to the solution composition and membrane characteristics. For example, for a

This journal is © The Royal Society of Chemistry 20xx

solution of a single monovalent salt (such as NaCl) of concentration C_s and a membrane of fixed charge density X, SDE relation will be as follows

$$\ln\left[\Gamma_s C_s \left(X+\Gamma_s C_s\right)\right]+\frac{\Delta W_s}{kT}=2\ln\left[\Phi_s C_s\right], \quad (2)$$

where Φ_s = $(\Phi_+\Phi_-)^{0.5}$ is the salt steric exclusion coefficient (average of the cation and anion) and $\Delta W_s=\Delta W_+ + \Delta W_-$. When $X >> \Gamma_s C_s$, i.e., the membrane charge is large compared with invading salt, an explicit solution of (2) is

$$\Gamma_s \approx \frac{\Phi_s^2 C_s}{X}\exp\left(-\frac{\Delta W_s}{kT}\right), \quad (3)$$

Relations (2) and (3) are easily generalized to multivalent salts and mixtures and may be used to relate salt exclusion to physical characteristics, entering through parameters X and ΔW_s. They also indicate that salt partitioning is inherently concentration-dependent.

We reiterate that the mean-field equations (2) and (3) imply that all ions are subject to the same mean-field Donnan potential. This assumption may break down in many cases, e.g., in channels wider than Debye length[29] or when ion non-ideality, e.g., ion correlations[30] or association[24] (see Section 2.4) are significant. As a result, even for strongly charged pores, the dependence may deviate from the linear relation $\Gamma_s \propto C_s$ suggested by (3). In such cases, the effective values of X and ΔW_s will vary with C_s as well. Nevertheless, (2) and (3) may be useful guiding relations, whenever variation of X and ΔW_s can be estimated or modelled, as elaborated next.

2.3. Relation of selectivity to physical characteristics

The classical Born equation[31] is commonly used to obtain realistic estimates of W and connect it to the characteristics of the ion and medium. It ignores inter-ionic interactions and integrates the electrostatic energy density around a lone ion in an infinite dielectric continuum to yield

$$\frac{W_\pm}{kT}=\frac{z_\pm^2 e^2}{8\pi\varepsilon_0\varepsilon r_\pm kT}\equiv\frac{1}{2}\frac{z_\pm^2\lambda_B}{r_\pm}\equiv\frac{1}{T^*}, \quad (4)$$

where z and and r are the charge (in units of electron charge e) and radius of the ion, ε is the dielectric constant. The last two relations define the Bjerrum length λ_B and reduced temperature T^* of the medium. In water $\lambda_B \approx 0.7$ nm and $T^* \sim 1$ for most ions, but when ε drops to 10, which corresponds to a mildly hydrophobic or moderately hydrated medium, λ_B increases to 5 nm and T^* becomes small ($T^* << 1$).

Experimentally measured ΔW for different ions in water relative to vacuum are best matched by so-called Born ion radii, which are only slightly larger than bare radii, but not as much correlated with corresponding Stokes radii.[32] The Born or bare radii then seem to be the most appropriate choice for calculating W in low-ε media. Given r's are typically 0.1-0.2 nm, for ε = 10 the exponential factor in equation (3) may be as small as 10^{-5} for monovalent ion and even 10^{-10} for divalent ions or still lower ε. This may be compared to the effect of X, whose nominal values rarely exceed 1 M in membranes.[33] Even for C_s as low as 10 mM, the Donnan exclusion factor C_s/X will only be about 10^{-2}, which is clearly insufficient to reach the aforementioned target of selectivity.

This simple argument emphasizes that the reliance on fixed charges alone is insufficient and it is critical to employ the dielectric mechanism as well. That latter can not only work on its own, as it does in case of cellulosic membranes,[18] but can also enhance the other mechanisms, as equation (3) emphasizes. Incidentally, that may be the case for in aquaporin channels as well, since the low-dielectric material that surrounds the charged constriction should raise the energy of charge repulsion.

In water-filled channels or nanopores, even for a lone ion, the situation becomes more complex. The simple Born equation is no more valid, since the polarization of pore-matrix interface by the ion (cf. image charges) modifies the self-energy in a strongly pore geometry-dependent manner. [17, 18, 30, 34-36] Yaroshchuk[20] reviewed the problem, giving expressions for pores of different geometries, including charged pores. In general, compared with non-porous matrix, W is reduced in a pore by a term inversely proportional to the pore size for a given pore geometry. The dielectric exclusion then rapidly weakens with increasing pore size, which may be readily misinterpreted as a signature of steric exclusion.

The above analysis indicates that best recipe for creating a highly selective channel is to *make the pore as small as possible AND ensure the pore environment be as low-dielectric as possible.* For instance, the relatively slow r^{-2} decay of the electrostatic energy density around an ion implied in derivation of (4) suggests that, as well as pore walls, fairly distant pore surrounding may have some effect on ion exclusion. Obviously, tuning dielectric properties, i.e., hydrophobicity/hydrophilicty of the pore, requires some care, since a hydrophobic pore may eventually become impermeable to water. The channel should then be as narrow and hydrophobic as possible yet *still allow fast water permeation*.

On the other hand, *tuning channel charge alone is insufficient for having a high selectivity*, even though it may enhance and tune salt rejection and perhaps help keep the pore water-permeable too. However, keeping a significant pore charge in a low-dielectric environment may not be straightforward, since much of the charge may become associated and inactive, as explained in the next section.

2.4. Ion association

Apart from non-trivial relations to pore geometry, another complex aspect of dielectric exclusion is its intimate relation to the effects, responsible for strong deviations from mean-field, in particular, ion sorption and association. Such effects, invalidating the mean-field approach, are controlled essentially by the same parameters as the self-energy, namely, charge and

size of the ions and dielectric constant of the medium, or, compactly, by *T**. The consequences are most dramatic in charged low dielectric media, i.e., exactly in the conditions desired for maximal selectivity.

To illustrate the point, we may adopt the same picture, as in derivation of equation (4), and consider hard-ball ions of the same size and absolute charge in a dielectric continuum. In this model, known as restrictive primitive model (RPM), the association constant for ion pairs is[37]

$$K \cong 4\pi b^3 T^* \exp\frac{1}{T^*}, \quad (5)$$

where $b = r_+ + r_- = 2r$ is the distance of closest approach in the pair. The low-dielectric conditions correspond to $T^* << 1$, in which case the missing numerical factor in (5) is close to 1.[37]

For simplicity, let us neglect the small self-energy in water and steric exclusion, i.e., assume that $\Delta W_s / kT \approx 2/T^*$ and $\Phi_s \approx 1$. Without fixed charge ($X = 0$), equation (2) yields

$$\Gamma_s = \Gamma_\pm \cong \exp\left(-\frac{1}{T^*}\right) \ll 1, \quad (6)$$

This means that for $T^* \ll 1$ the ion concentration in the membrane $\Gamma_s C_s$ will be small. The fraction of associated ions is given by

$$\frac{K(\Gamma_s C_s)^2}{\Gamma_s C_s} = K\Gamma_s C_s \cong C_s b^3 T^* \ll 1. \quad (7)$$

This means that in a non-charged low-dielectric membrane the small fraction of ion pairs will be small and contribute negligibly to salt transport, as was long ago established for lipid membranes.[36]

However, if the membrane contains a *large* fixed charge *X*, it will also have to contain an equivalent concentration of counter-ions, a substantial fraction of which may associate. Roughly, this will happen when the Bjerrum length λ_B exceeds the spacing of ionic groups, thus electrostatics starts dominating over thermal motion. A certain similarity may be seen with the well-known Manning counter-ion condensation on linear charges (polyelectrolytes),[38] however, the analogy is superficial, since the parameters controlling the residual effective charge are different.

For the present case of discrete fixed charges dispersed in 3D, consider the relation between the residual fixed charge density X_{ef} and the total fixed charge *X*. Since the concentration of free non-associated counter-ions is X_{ef} as well, the association equilibrium reads

$$X_{ef} = \frac{X}{1 + KX_{ef}}. \quad (8)$$

If the association constant is small, $KX_{ef} \approx KX \ll 1$, the effective charge is not much different form the total one $X_{ef} \approx X$. However, if association constant is large, $KX_{ef} \approx KX \ll 1$, eq. (8) becomes

$$X_{ef} \approx \frac{X}{KX_{ef}}. \quad (9)$$

whence the effective fraction of the fixed charge is approximately

$$\frac{X_{ef}}{X} \approx (XK)^{-1/2} \cong (Xb^3)^{-1/2} T^{*-1/2} \exp\left(-\frac{1}{2T^*}\right). \quad (10)$$

This indeed becomes small, when *T** is small enough.

The resulting X_{ef} then replaces *X* in equation (3), which shows that salt partitioning is affected by T^* in two ways, through X_{ef} and W_s. Ultimately, this yields a weaker exclusion, with a more complex dependence on *T** and a weaker dependence on the nominal fixed charge *X* than equation (2), as follows

$$\Gamma_s \approx \frac{C_s}{X_{ef}} \exp\left(-\frac{2}{T^*}\right) \approx \frac{C_s b^{3/2}}{X^{1/2}} T^{*1/2} \exp\left(-\frac{3}{2T^*}\right). \quad (11)$$

The last four relations imply that the mean-field (Donnan) potential still apples to non-associated ions, in the spirit of Bjerrum's treatment of ion association.[39] However, it no more applies to associated ions, since mean field cannot adequately describe strong and rapidly varying potential around fixed charges, leading to strong spatial correlations between the fixed charges and counter-ions and their immobilization.

Deviations from mean-field, implied in Donnan or Poisson-Boltzmann models, are usually significant in aqueous solutions only for multivalent ions.[40] They manifest themselves in effects such as surface charge reversal or layering, which can be viewed as weak forms of association and require introducing non-field elements in the models.[34, 40-42] Here we see that in highly selective membranes such effects can be strong even for monovalent ions, as our recent MD simulations of polyamide membranes demonstrate.[15] For this reason, in order not to overestimate ion exclusion, the Poisson-Boltzmann description that has been widely used for modelling charged nanochannels, [29, 42-44] must be modified for in narrow and highly selective water channels that employ low-T^* regimes. Incorporation of association equilibria into such models as a way to calculate an effective charge might offers a simple phenomenological way to address such deviations.

2.5. Specific ion sorption in polymers and nanotubes

2.5.1. Polymeric membranes

The previous section highlights the role and importance of ion association in low-*T** membranes and nanochannels. However, strong ion-specific interactions, absent in RPM but present in real systems, can substantially modify ion exclusion relation even at moderate *T**. Ions that may be particularly prone to such behaviour are H^+ and OH^-, inherently present in any aqueous system. Apart from being uniquely small, which facilitates association, these ions may readily form hydrogen-

This journal is © The Royal Society of Chemistry 20xx

and even covalent bonds with many chemical groups and water within membranes or channels. A best-known example is binding of H^+ by weakly acidic carboxylic groups. Due to covalent bonding, its association constant in water is 10^4 M^{-1} (pK_a ~ 4), many orders of magnitude stronger than purely electrostatic association. In desalination membranes pK_a of carboxylic groups was shown to shift several orders of magnitude up to ~8-9.[45] The extra self-energy of the fixed carboxylic charges W ~ 10 kT removed upon protonation explains this shift. Equation (4) with appropriate values of r and λ_B well agrees with this W.

Recent studies demonstrate that specific ion binding or sorption may not even require a large X and be remarkably strong even in nominally neutral low-T^* materials, lacking any acidic or basic binding sites. This is most readily revealed by analysing the membrane conductance. Indeed, the specific conductance Λ of a polymer equilibrated with an ionic solution is directly connected to ion permeabilities and, ultimately, to ion diffusivities and partitioning, as follows[46]

$$\Lambda = \frac{F^2}{RT}\sum_i P_i C_i z_i^2 = \frac{F^2}{RT}\sum_i D_i \Gamma_i C_i z_i^2 \quad , \qquad (12)$$

where summation is over all ions in solutions and P's are area- and thickness-normalized. Unlike the salt permeabilities determined by the least-permeating ion of the salt, Λ is controlled by the fastest permeating ion, offering a complementary insight into ion permeation.

Our recent results on ion conductance of polyamide membranes and Nomex films, known to have a high water-salt selectivity, reveals strong affinity affects.[24, 47] The conductance of Nomex films immersed in solutions of different chloride salts, covering a 3 orders of magnitude C_s range, showed an unusual 1/2-power scaling of conductivity[24, 47]

$$\Lambda \propto C_s^{1/2} \quad , \qquad (13)$$

Curiously, the measured dependence was virtually independent of cation type, except for HCl solutions that showed the regular linear scaling $\Lambda \propto C_s$. The conductivity for salts was also pH-dependent, increasing by about an order of magnitude when pH dropped by 2 units. This strongly suggests that, despite the very low H^+ concentration in solution, the neutral combination that the polymer uptakes is always HCl and not metal salts MCl or MCl_2, thereby one has

$$\Gamma_{M^+} C_{M^+} \ll \Gamma_{H^+} C_{H^+} \approx \Gamma_{Cl^-} C_{Cl^-} \propto \left(C_{H^+} C_{Cl^-}\right)^{1/2} = 10^{-pH/2} C_s^{1/2} \quad , \qquad (14)$$

in agreement with (13). Such a behavior then indicates an exceptionally high affinity of Nomex to protons. The crossover to $\Lambda \propto C_s$ at high C_s let us estimate that proton affinity to polyamide was about 10^3 times that of Na^+ and >10^7 times that of Ca^+, which is far beyond simple electrostatics. Presumably, the reason for such exceptional affinities is, on one hand, strong dielectric exclusion of salt cations and, on the other hand, strong and specific proton-polymer interactions.

The effect of H^+ uptake is equivalent to formation of a positive effective "fixed" charge X_{ef}. However, due to the need to take up an equivalent amount of anions and compete with other cations, the charge is not "fixed" and depends on both pH and C_s. Formation of such positive charge may have a significant impact on both permselectivity and salt permeation. An increase in positive charge will always facilitate anion permeation and hold back cations. The ultimately effect will then depend on which ion controls salt permeation. For instance, If the membrane is inherently more permeable to the anions than cations, proton uptake (lower pH) will increase salt permeability, yet it will do the opposite if the membrane is preferentially permeable to cations. [24, 48]

2.5.2. Carbon nanotube channels

A behaviour that resembles that of Nomex was reported for conductivity of CNT nanochannels, however, the interpretation brought up much controversy. For wider nanotubes, where screening effects come into play, Secci at al proposed a model that predicts an unusual scaling $\Lambda \propto C_s^{1/3}$ that seemed to conform to their data. [44] The proposed mechanism assumed that the charge-generating mechanism in CNTs was specific adsorption of OH^- ions, which rendered the channel negatively charged. The model was, however, criticized by Biesheuvel and Bazant,[29] who pointed out that it relied on two physically incompatible assumptions. Instead, they proposed an *ad hoc* Langmuir-type OH adsorption thus the trend observed by Secci et al. was interpreted as a transition between adsorbed charge saturation regime $\Lambda \propto C_s^0$ and linear high-salt regime $\Lambda \propto C_s^1$. Curiously, Biesheuvel and Bazant also pointed out a possibility of $C_s^{1/2}$ scaling at unattainably low C_s. Nevertheless, such scaling was reported for C_s ranging from <0.01 M to >1 M by Tunuguntla et al. [6] for short (~12 nm) 0.8-nm CNTs, as well as by Amiri et al.[2] for 20 μm-long 1.5-nm CNTs. These authors attributed the observed scaling to progressively screened carboxylic charges at the nanopore rims. This conclusion was based on the drop in conductance and transition to regular C_s^1 scaling below pH 5, close to pK_a of carboxylic groups. Yet, it is surprizing that the effect of rim charges, which is supposed to extend over a few nanometers and is thus likely for short CNTs used by Tunuguntla et al., could as well control the transport in much longer CNTs in experiments by Amiri et al. Besides, maintaining $C_s^{1/2}$ scaling without saturation over such a wide C_s range is less likely for genuine fixed charges (carboxyls) at the rim that directly faces aqueous environment.

This controversy will have to be resolved in the future, but it may be noted that the above data and other results discussed in these reports might be well explained by competitive adsorption of OH^- on CNT walls. This should be aided by strong dielectric exclusion of salt cations, in a manner similar to H^+ uptake in Nomex. For instance, the crossover at pH~5 could simply correspond to the isoelectric point (pI), at which the

large affinity of CNT walls to OH^- no more compensates for the drop in OH^- concentration, thus H^+ and/or salt take over. Note that a similar pI is often observed for many uncharged hydrophobic surfaces in water.[49]

The results for CNTs therefore indicates that, just as in polymeric membranes, charge control in highly selective (i.e., strongly salt- and ion-excluding) channels, is likely to encounter a specific adsorption of H^+ and OH^- ions. This may modify the channel selectivity in a complex way that may depend on the channel chemistry, solution composition and pH.

As a final note, the reported transport data for 0.8-nm CNTs[6] allow estimating the level of water-ion selectivity achievable today in CNT channels. At conditions roughly matching seawater, 0.5 M KCl and pH 7.5, 0.8-nm CNTs showed a conductance G ~ 50 pS and K^+/Cl^- selectivity ~200:1. This translates to the channel permeability to KCl, controlled by chloride, as follows

$$\frac{GRT}{200F^2C_s}=\frac{50\cdot10^{-12}\times2.5\cdot10^3}{200\times(10^5)^2\times0.5\cdot10^3}\approx10^{-22}\ \ m^3/(s\times channel)$$

.

On the other hand, the osmotic water permeability, measured using stop-flow technique for the same CNTs at 0.6 M NaCl and pH 7.8 was found to be about $P_w\sim10^{-18}\ \mathrm{m^3/(s\times channel)}$. That yields a selectivity factor $\alpha_P\sim10^{-4}$, which misses by just an order of magnitude the 10^{-5} target set by today's commercial desalination membranes. Since 0.8-nm tubes are still not the narrowest possible, this result should be seen as encouraging, provided the challenge of concentration polarization, analysed in the next section, is addressed.

3. Concentration polarization: the case of water channels

3.1. Polarization relations for planar membranes

Concentration polarization (CP) refers to the mass transfer resistances associated with unstirred solution layers adjacent to a selective membrane, turning the membrane into an inferior "multilayer". Its impact is nearly always detrimental and undesired and is two-fold. First, the added resistance slows-down the permeation rates. Second, the solution layer, lacking selectivity, reduces overall selectivity of the "multilayer".

A major limitation on the overall permeation rate (flux or current) is set by the diffusion permeability of the unstirred boundary layer D/δ, commonly called the boundary layer mass transfer coefficient, where δ is the boundary layer thickness and D is the relevant diffusivity. For macroscopic membranes, hydrodynamic conditions largely determine δ and reducing it below 10 μm requires high-shear flows, which weighs excessively on the energy consumption. As a result, δ is normally in the range 10-50 μm thereby D/δ rarely exceeds 20-30 μm/s. An attempt to increase water flux or ion current beyond this rate by increasing the driving force, e.g., pressure or electric potential, will result in a loss of most driving force within the unstirred layer. This general argument applies to all membrane processes, however, the effect on permeation and selectivity and the parameters controlling CP may somewhat differ, depending on the specific process.

In osmotic processes, it is customary to use water and salt permeability coefficients A and B related to permeabilities P_w and P_s defined *per unit membrane area*, as follows[50]

$$A=\frac{P_wV_w}{RT},\ B=P_s \qquad (15)$$

where V_w is the water molar volume. Typical values for modern reverse osmosis (RO) membranes are of the order A ~ 1 μm/(s×bar) and B ~ 10^{-2} μm/s, which is what sets the target value for the selectivity α_p ~ 10^{-5}. In RO, water volume flux J_w may be viewed as an independent operational variable controlled by the applied pressure ΔP_{net} (applied pressure minus osmotic pressure difference), $J_w=A\Delta P_{net}$. To obtain the steady-state salt flux J_s for a given J_w, salt permeation through the membrane has to match convection-diffusion in the upstream boundary layer. For regular planar membranes, only the dimension normal to the membrane surface (x) need to be considered, as follows[21]

$$J_s=B\left(C_m-C_p\right)=-D_s\frac{dC}{dx}+J_wC \qquad (16)$$

where C_m is the concentration at the feed-membrane interface and $C_p = J_s/J_w$ is the permeate concentration. Solution of (16) shows that the observed salt permeability will be larger than the "ideal" permeability B,

$$B_{obs}=B\exp\left(\frac{\delta}{D_s}J_w\right) \qquad (17)$$

This is a result of the exponential growth of C_m, which will also increase the osmotic difference and prevent increase of J_w much beyond diffusion permeability of the boundary layer D_s/δ, when applied pressure increases.

Situation is different in forward osmosis (FO), where the same salt concentration difference between brine (b) and diluate (d) drives both water and salt in opposite directions.[51] As a result, the virtual "permeate" concentration $C'_p=J_s/J_w=B/ART$ is fixed by the ratio of permeabilities B/A, regardless of CP. However, CP will greatly affect the fluxes. Coupling the convection-diffusion in two unstirred layer on b and d sides with permeation through the membrane yields an implicit relation for J_w

$$J_w=ART\left\{\left(C_b+C'_p\right)e^{-\frac{\delta_b}{D}J_w}-\left(C_d+C'_p\right)e^{\frac{\delta_d}{D}J_w}\right\} \qquad (18)$$

Solution of (18), illustrated in Figure 1, shows that (a) CP reduces the osmotic driving force below the ideal value $C_b - C_d$, and (b) there is an upper limit for achievable water flux, determined by the combined diffusion resistance of both unstirred layers and membrane selectivity (C'_p), as follows

This journal is © The Royal Society of Chemistry 20xx

$$J_{w,\lim} = \frac{D}{\delta_b + \delta_d} \ln \frac{C_b + C'_p}{C_d + C'_p} \quad (19)$$

Note that δ_b or δ_d may contain the resistance of porous supporting layers of the membrane as well ("structure factor"[51]).

Finally, consider an electric current through an ion-selective membrane surrounded by a (monovalent) salt solution of concentration C_s and diffusivity D_s. At one side, the membrane-solution interface will get progressively depleted of salt and the potential drop will exponentially increase, when current density approaches the limiting density given by[52]

$$i_{\lim} = \frac{FD_sC_s}{\delta(t_m - t_s)}, \quad (20)$$

where t_m and t_s are the counter-ion transference numbers for the membrane and solution. Here the relevant diffusion resistance $\delta(t_m - t_s)/D_s$ limits the rate of supply of co-ions to the membrane surface, which is necessary to prevent inifinte increase of potential drop.

The above limitations imposed by CP have been well recognized as critical for conventional planar membranes. They may however change significantly for water channels. This aspect may be particularly critical for scale-up from individual channels or pore-spanning membrane patches or vesicles of microscopic size to macroscopic channel arrays, which may result in a drastic change in CP conditions, as discussed in the next section.

3.2. Channels and channel-array membranes

3.2.1. Polarization in an isolated channel

Electrochemists were perhaps the first to recognize the phenomenon of polarization, which bears much similarity between solid electrodes and perm-selective membranes. They also came up with a way to reduce polarization and decouple it form hydrodynamics by using microelectrodes of lateral dimensions much smaller than the unstirred layer thickness δ.[53]

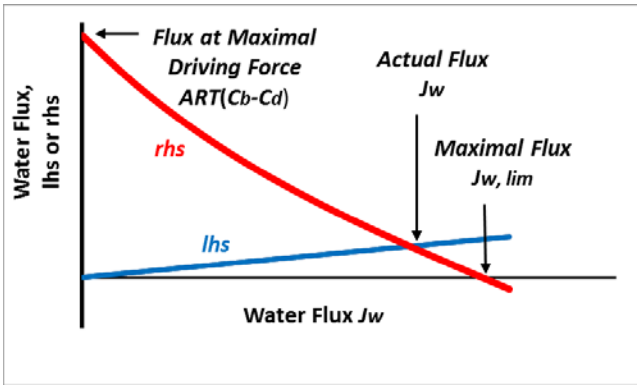

Figure 1. Graphical solution of equation (18): The blue and red lines represent left- and right-hand sides of (18); their intersect gives the actual flux under given CP conditions. The intersect of rhs line and Y-axis corresponds to the flux at negligible CP, when the entire driving force falls on the membrane. The intersect of the rhs line and X-axis corresponds to the limiting flux given by equation (19), when membrane permeability A is infinitely large.

Nanoscopic channels embedded in an impermeable membrane, e.g., a lipid bilayer, are analogues of microelectrodes, as much as conventional membranes are analogues of planar electrodes. What makes the major difference between a channel and a macroscopic membrane is the fact that a *semispherical diffusion field* centered at the channel mouth will replace the planar boundary layer (cf. Figure 2a and b). As a result, for RO, the radial coordinate r and flow rates Q will replace coordinate x and fluxes J in (1) to yield[54]

$$Q_s = P_s(C_m - C_p) \approx -2\pi r^2 D_s \frac{dC}{dr} + Q_w C \quad (21)$$

Note that, from here on, P_w and P_s are redefined *per channel.* Solving (21) replaces (17) with

$$P_{s,obs} \approx P_s \exp\left(\frac{Q_w}{2\pi D_s R_c}\right), \quad (22)$$

where R_c is the channel radius, which is assumed to be much smaller than the outer radius R_o of the diffusion profile, i.e., the "thickness" of the diffusion profile in Fig. 2b, at which C equals the bulk concentration C_b. Similar to δ, the value of R_o is determined by hydrodynamic mixing conditions, $R_o \sim \delta$. However, since $\delta >> R_c$, hydrodynamics has essentially no effect on observed permeability for a single channel.

For FO, (18) and (19) are similarly replaced with relations

$$Q_w \approx P_w V_w \left\{ (C_b + C'_p) e^{-Q_w/2\pi D_s R_c} - (C_d + C'_p) e^{Q_w/2\pi D_s R_c} \right\}, \quad (23)$$

$$Q_{w,\lim} = \pi D_s R_c \ln \frac{C_b + C'_p}{C_d + C'_p}. \quad (24)$$

Finally, the limiting current $I_{\lim}$ for ion-selective microchannel will be

$$I_{\lim} \approx \frac{2\pi R_c F D_s C_s}{t_m - t_s}. \quad (25)$$

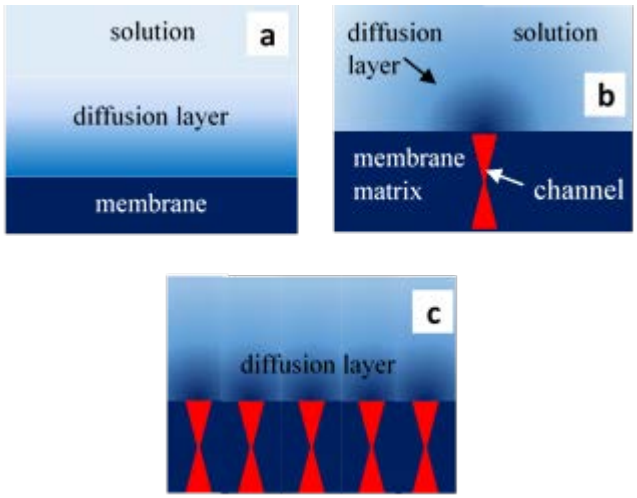

Figure 2. Concentration polarization and the geometry of the diffusion field in solution adjacent to (a) a planar homogeneous membrane, (b) an isolated single channel, (c) closely spaced channel array with overlapping diffusion layers.

The limitations set by equations (22), (24) and (25) are significantly less restrictive than for their planar membrane counterparts (17), (19) and (20). The aforementioned data by Tunuguntla et al. on 0.8 nm CNT channels (R_c = 0.34 nm)[6] may be used to illustrate the point. For the reported permeability $P_w \sim 10^{-18}$ m^3/s/channel, even if one takes the osmolarity difference C_s as high as 1 M to maximize Q_s, the term under exponents in equation (23) will be

$$\frac{Q_w}{2\pi R_c D_s} = \frac{P_w V_w C_s}{2\pi R_c D_s} \sim \frac{10^{-18} \times 1.8 \cdot 10^{-5} \times 10^3}{2\pi \times 0.34 \cdot 10^{-9} \times 1.5 \cdot 10^{-9}} \approx 0.006,$$

which indicates a negligible CP.

Similarly, the maximal current employed in potential reversal experiments with C_s = 1 M at the dilute side was of the order 10 pA, whereas equation (25) estimates the limiting current as

$$I_{\lim} \sim \frac{2\pi \times 0.4 \cdot 10^{-9} \times 10^5 \times 1.5 \cdot 10^{-9} \times 10^3}{1 - 0.5} \approx 2 \cdot 10^{-9} A \approx 2\ nA,$$

i.e., three orders of magnitude larger, indicating a negligible effect of polarization on the measurements.

3.2.2. Channel arrays: vesicles, nanopores, and macroscopic membranes

In foreseeable implementation scenarios, scaled-up devices will require arrays of channels embedded in a macroscopically large membrane. Unfortunately, the negligible effect of polarization on isolated individual channels, highlighted in the previous section, may no more apply to such arrays. The spherical symmetry of the diffusion fields around individual channels will transition to the regular planar one, once the fields of neighboring channels begin to overlap within the unstirred layer (Figure 2c). The limiting flux or current is then anticipated to drop substantially already at $L \sim \delta$, where L designates the average spacing of the channels. The analysis of microelectrode arrays indicates that the behavior of an array will be indistinguishable from a planar membrane for $L < \delta/3$.[53]

The water flux per total footprint area of a channel array is related to the permeation rate per channel as

$$J_w = Q_w L^{-2}. \quad (26)$$

The need to maximize the flux is an incentive to minimize L, i.e., increase channel density. However, once L in an array drops under δ, the limiting values of flux or current per channel will also drop relative to an individual channel by a factor, cf. equations (19), (24) and (26),

$$\frac{Q_{w,\lim} L^2}{J_{w,\lim}} \cong \frac{L^2}{\delta R_c}. \quad (27)$$

This factor can still make no difference for arrays inserted in membranes of microscopic area, such as vesicles employed in stop-flow experiments or membrane patches spanning a single nanopore for membrane potential and current measurements.[6] In such cases the planar diffusion field at distances less than the membrane size will transition to semi-spherical at larger distances. This means that the effective boundary layer thickness in such cases will correspond to the radius of the vesicle or nanopore membrane R_m, typically ranging from 50 to 1000 nm.

As an example, take $L \sim 10^{-8}$ m (10 nm), corresponding to a maximal density of aquaporins in living cell membranes,[55] which is obviously much smaller than the membrane size R_m. Packing 1-nm channels ($R_c = 5\times10^{-10}$ m) in a vesicle even as large as $R_m \sim 5\times10^{-7}$ m (500 nm, typical of many living cells) yields

$$\frac{L^2}{R_m R_c} \sim (10^{-8})^2 / (5 \cdot 10^{-7} \times 5 \cdot 10^{-10}) \sim 0.4 \cdot$$

This is an insignificant factor therefore CP is nearly as negligible as in a single channel. Channels in vesicles or nanopores then negligibly interfere with each other, as aquaporins apparently do in living cells, and are subject to negligible CP. Importantly, since $R_m << \delta$, hydrodynamics has no or little effect on CP.

However, in a macroscopic planar array of such density, an opposite relation $R_m >> \delta$ holds, therefore the flow-dependent unstirred layer thickness $\delta \geq 10^{-5}$ m (10 μm) rather than membrane size will determine the limiting rate. The latter will then drop, relative to a single channel, by a factor

$$L^2/\delta R_c \leq (10^{-8})^2 / (10^{-5} \times 5 \cdot 10^{-10}) \sim 0.02 \cdot$$

This >50-fold drop in limiting flux J_{lim}, going under exponent as J_w/J_{lim}, may increase CP to an extent that the selectivity estimated for an isolated channel may be impossible to achieve in a membrane for any reasonable J_w.

As another example, consider the density of CNT porins used by Tunungutla et al., which was 5-30 channels per 200 nm vesicle,[6] corresponding to $L \sim 10^{-7}$ m (100 nm). For this value and $\delta \sim 10$ μm, $L^2/\delta R_c \sim 1$, i.e., packing channels in a planar array of such density will not make a difference in CP, compared with an isolated channel. However, such a low-density array had a fairly low water permeability

$$A = \frac{P_w V_w}{L^2 RT} = \frac{10^{-18} \times 1.8 \cdot 10^{-5}}{(10^{-7})^2 \times 2.5 \cdot 10^3} < 10^{-12}\ m/s/Pa,$$

which is too small, compared with today's RO membranes, $A \sim 5 \cdot 10^{-12}$ m/s/Pa. An attempt to increase density to match this A will reduce J_{lim} by the same factor and exponentially increase CP.

Apparently, the problem of CP in macroscopic channel array membranes have no easy solution. The present analysis suggests that a careful optimization of the channel density may be required, still subject to fundamental upper limitation. When osmotic pressure is not large, e.g., in purification of low-salinity feeds, very high channel selectivity may compensate for CP-enhanced salt permeation and allow some increase in water permeation rates. This re-emphasizes the importance of maximizing the channel selectivity.[11] In either case, the current polymeric membranes remain tough competitors for artificial channels, in terms of both selectivity and permeability.[56]

This journal is © The Royal Society of Chemistry 20xx

Conclusions

In foreseeable applications, the selectivity of artificial water channels may be as important as water permeability, yet at present, it is about an order of magnitude off the target set by today's polymeric membranes. The lessons learned from conventional membranes suggest that dielectric mechanism is the one that is most likely to deliver the desired selectivity. To achieve the required effect, it is equally crucial to have the channels both narrow and surrounded by a low-dielectric environment in order to raise the ion self-energy. In contrast, pore charge is apparently insufficient on its own to reach the required strength of exclusion. However, charges may help enhance and tune ion rejection, provided non-mean-field effects, such as ion sorption and association enhanced in low-dielectric pores, especially of H^+ and OH^- ions, are properly understood and addressed. As discussed here, such effects may significantly modify the pore charge and thus increase or decrease selectivity.

Another important point, well recognized in membrane science and analyzed here in the context of water channels, is the effect of concentration polarization. The presented analysis shows that the CP level is apparently always small in experiments with individual channels or microscopically small membranes. However, the situation may drastically change in macroscopic membranes incorporating densely spaced channel arrays, due to a different geometry of the diffusion field. As a result, projections from microscopic experiments to macroscopic membranes runs the risk of overestimating their potential performance. If not properly addressed in membrane design, the increased CP level in scaled-up channel-based membranes may significantly compromise the observed selectivity and require that the target of selectivity be re-set to a still more challenging level.

The points highlighted in this paper may help guide future development of high-performance artificial water channels and their scale-up towards utilization in next-generation desalination and water purification membranes.

Conflicts of interest

The author declares no conflicts of interests.

Acknowledgements

The financial support by Israel Science Foundation (grant #1152/11) and by a joint grant 2016627 of the United States-Israel Binational Science Foundation (BSF), Jerusalem, Israel, and United States National Science Foundation (NSF) is acknowledged. The author thanks Dr. Aleksandr Noy (LLNL and UC Merced) and Prof. Meni Wanunu (Northeastern U) for many illuminating discussions and for sharing data prior to publication.

References

1. P. Agre, *Proceedings of the American Thoracic Society*, 2006, **3**, 5-13.
2. H. Amiri, K. L. Shepard, C. Nuckolls and R. l. Hernández Sánchez, *Nano Lett.*, 2017, **17**, 1204-1211.
3. M. Barboiu, *Angewandte Chemie International Edition*, 2012, **51**, 11674-11676.
4. Y.-x. Shen, P. O. Saboe, I. T. Sines, M. Erbakan and M. Kumar, *J. Membr. Sci.*, 2014, **454**, 359-381.
5. Y.-x. Shen, W. Si, M. Erbakan, K. Decker, R. De Zorzi, P. O. Saboe, Y. J. Kang, S. Majd, P. J. Butler, T. Walz, A. Aksimentiev, J.-l. Hou and M. Kumar, *Proceedings of the National Academy of Sciences*, 2015, **112**, 9810-9815.
6. R. H. Tunuguntla, R. Y. Henley, Y.-C. Yao, T. A. Pham, M. Wanunu and A. Noy, *Science*, 2017, **357**, 792.
7. B. J. Hinds, N. Chopra, T. Rantell, R. Andrews, V. Gavalas and L. G. Bachas, *Science*, 2004, **303**, 62-65.
8. J. K. Holt, H. G. Park, Y. Wang, M. Stadermann, A. B. Artyukhin, C. P. Grigoropoulos, A. Noy and O. Bakajin, *Science*, 2006, **312**, 1034-1037.
9. J. Abraham, K. S. Vasu, C. D. Williams, K. Gopinadhan, Y. Su, C. T. Cherian, J. Dix, E. Prestat, S. J. Haigh and I. V. Grigorieva, *Nature nanotechnology*, 2017, **12**, 546-550.
10. D. Cohen-Tanugi and J. C. Grossman, *Nano Lett.*, 2012, **12**, 3602-3608.
11. J. R. Werber, A. Deshmukh and M. Elimelech, *Environmental Science & Technology Letters*, 2016, **3**, 112-120.
12. F. Fornasiero, H.-G. Park, J. K. Holt, M. Stadermann, C. Grigoropoulos, A. Noy and O. Bakajin, *Proc. Natl. Acad. Sci. USA*, 2008, **105**, 17250-17255.
13. B. Corry, *Energy & Environmental Science*, 2011, **4**, 751-759.
14. M. Ding, A. Szymczyk, F. Goujon, A. Soldera and A. Ghoufi, *J. Membr. Sci.*, 2014, **458**, 236-244.
15. V. Kolev and V. Freger, *J. Phys. Chem. B*, 2015, **119**, 14168-14179.
16. Y. Luo, E. Harder, R. S. Faibish and B. Roux, *J. Membr. Sci.*, 2011, **384**, 1-9.
17. L. Dresner, *Desalination*, 1974, **15**, 371-374.
18. E. Glueckauf, *Desalination*, 1976, **18** 155-173.
19. A. Szymczyk, N. Fatin-Rouge, P. Fievet, C. Ramseyer and A. Vidonne, *J. Membr. Sci.*, 2007, **287**, 102-110.
20. A. E. Yaroshchuk, *Adv. Colloid Interface Sci.*, 2000, **85**, 193-230.
21. M. H. V. Mulder, *Basic Principles of Membrane Technology*, Kluwer Academic, Dordrecht, The Netherlands, 1996.
22. M. Chaplin, Water Molecule Structure, http://www1.lsbu.ac.uk/water/water_molecule.html#g, (accessed March 1, 2018).
23. F. Franks, *Water: a matrix of life*, Royal Society of Chemistry, 2007.
24. N. Fridman-Bishop, K. A. Tankus and V. Freger, *J. Membr. Sci.*, 2018, **548**, 449-458.
25. Y. Lanteri, P. Fievet and A. Szymczyk, *J. Colloid Interface Sci.*, 2009, **331**, 148-155.
26. S. Levchenko and V. Freger, *Environmental Science & Technology Letters*, 2016, **3**, 339-343.
27. A. E. Yaroshchuk, *Sep. Purif. Tech.*, 2001, **22-3**, 143-158.
28. J. Giddings, *J. Phys. Chem.*, 1968, **72**, 4397.

29. P. Biesheuvel and M. Bazant, *arXiv preprint arXiv:1610.01309*, 2016.
30. S. Buyukdagli, M. Manghi and J. Palmeri, *Phys. Rev. Lett.*, 2010, **105**, 158103.
31. M. Born, *Zeitschrift für Physik*, 1920, **1**, 45-48.
32. C. S. Babu and C. Lim, *Chem. Phys. Lett.*, 1999, **310**, 225-228.
33. L. A. Perry and O. Coronell, *J. Membr. Sci.*, 2013, **429**, 23-33.
34. S. Buyukdagli, M. Manghi and J. Palmeri, *The Journal of Chemical Physics*, 2011, **134**, 074706.
35. R. R. Netz, *J. Phys.: Condens. Matter*, 2003, **15**, S239.
36. A. Parsegian, *Nature*, 1969, **221**, 844-846.
37. J. N. Aqua, S. Banerjee and M. E. Fisher, *Phys. Rev. E*, 2005, **72**.
38. G. S. Manning and J. Ray, *J. Biomol. Struct. Dyn.*, 1998, **16**, 461-476.
39. R. A. Robinson and R. H. Stokes, *Electrolyte Solutions*, Dover Pubns, 2002.
40. A. Y. Grosberg, T. T. Nguyen and B. I. Shklovskii, *Rev. Mod. Phys.*, 2002, **74**, 329.
41. H. Boroudjerdi, Y.-W. Kim, A. Naji, R. R. Netz, X. Schlagberger and A. Serr, *Phys. Rep.*, 2005, **416**, 129-199.
42. D. Gillespie, *Nano Lett.*, 2012, **12**, 1410-1416.
43. J.-F. Pietschmann, M.-T. Wolfram, M. Burger, C. Trautmann, G. Nguyen, M. Pevarnik, V. Bayer and Z. Siwy, *Physical Chemistry Chemical Physics*, 2013, **15**, 16917-16926.
44. E. Secchi, A. Niguès, L. Jubin, A. Siria and L. Bocquet, *Phys. Rev. Lett.*, 2016, **116**, 154501.
45. O. Coronell, M. I. González, B. J. Mariñas and D. G. Cahill, *Environ. Sci. Technol.*, 2010, **44**, 6808-6814.
46. S. Bason, Y. Oren and V. Freger, *J. Membr. Sci.*, 2011, **367**, 119-126.
47. N. Fridman-Bishop and V. Freger, *J. Membr. Sci.*, 2017, **540**, 120-128.
48. O. Nir, N. F. Bishop, O. Lahav and V. Freger, *Water research*, 2015, **87**, 328-335.
49. K. N. Kudin and R. Car, *J. Am. Chem. Soc.*, 2008, **130**, 3915-3919.
50. A. Tiraferri, N. Y. Yip, A. P. Straub, S. R.-V. Castrillon and M. Elimelech, *J. Membr. Sci.*, 2013, **444**, 523-538.
51. T. Y. Cath, A. E. Childress and M. Elimelech, *J. Membr. Sci.*, 2006, **281**, 70-87.
52. K. Spiegler, *Desalination*, 1971, **9**, 367-385.
53. E. Gileadi, *Electrode Kinetics for Chemists, Chemical Engineers, and Material Scientists*, New York : VCH, 1993.
54. E. L. Cussler, *Diffusion: mass transfer in fluid systems*, Cambridge university press, 2009.
55. A. S. Verkman, *Current biology : CB*, 2013, **23**, R52-R55.
56. V. Freger, *Science*, 2015, **348**, 1317-1318.

This journal is © The Royal Society of Chemistry 20xx